

Proceedings of the Research Institute of Atmospheric,
Nagoya University, Vol. 36 (1989)

RESEARCH REPORT

PRELIMINARY LIDAR OBSERVATION OF TROPOSPHERIC OZONE PROFILE

H. Ishimaru*, A. Iwata, Y. Kondo, and M. Takagi

Abstract

A preliminary experiment of lidar observation was made to obtain the profile of the tropospheric ozone by the differential absorption technique. The system used consists of a tunable dye laser which operates in wavelengths 282–295 nm of Hartley ozone absorption band. It was confirmed that the reliable vertical profile was obtained in the altitude range 2–6 km from successive observations at two wavelengths separated with several nm.

1. Introduction

The atmospheric ozone has protected life on earth from harmful solar ultraviolet radiation through the long evolution of animals and plants. At the same time ozone has a key role in the thermal structure of the atmosphere and has an important relation to the human environment. The concentration of ozone depends on the balance between the photolytic generation from oxygen molecules due to solar UV radiation, the dissipation by reactions with some atmospheric minor species, and the dynamic transports. The tropospheric ozone budget is considered to be mainly controlled by the influx from the stratosphere, the destruction at the earth surface, as well as the photochemical generation and dissipation [Fishman *et al.*, 1985]. The mechanism of these processes is not yet fully understood in quantitative forms. On the other hand, the ozone is recognized to be a good tracer for atmospheric circulation and

* Now at Matsushita Electric Industrial Co., Ltd.

exchange between the stratosphere and troposphere. It is thus important to obtain the information on ozone distribution and its spatial and temporal variations.

This report is concerned with a preliminary experiment for observing the vertical profile of ozone by using the differential absorption technique of UV pulse lidar (DIAL). This technique has been actually utilized by some workers to monitor the ozone profiles up to the stratosphere [*Pelon and Megie, 1982; Megie et al., 1985*], and the errors in observations have also been discussed [e.g., *Schootland, 1984; Browell et al., 1985*].

2. Instrumentation

The basic construction of the used lidar system was reported by *Iwata et al. [1983]*. The installation used here is the second harmonic of tunable dye laser which is pumped by the second harmonic of Nd:YAG laser. The outline of laser transmitter composition is shown in Fig. 1. The main parts are Nd:YAG laser (Quantel YG481) and dye laser (Quantel TDL-IV) using the dye Rh6G in methanol solvent, and their specifications after careful tuning are given in Table 1. Figures 2 and 3 are, respectively, the wavelength characteristics of output powers of the fundamental and the second harmonic of dye laser. The powers were measured with a disk-calorimeter (Scientech Inc. Model 38-0101). In measuring the second harmonic power, a Pellin-Broca type prism was used to separate the fundamental, because the output from the second harmonic generator was the mixture of both fundamental and second harmonic. It is shown in Fig. 2 that the fundamental of the dye laser operates in laser mode in the wavelength range 564 – 590 nm, the peak power of which is 27 mJ/pulse at 570 nm. As shown in Fig. 3, the second harmonic, which is used for actual observation, is in the wavelength range 282 – 295 nm and the peak power is 2.7 mJ/pulse at 285 nm.

The laser system is installed horizontal, and a right-angle prism is inserted to emit the laser beam upward. The prism is made of compound quartz glass and its transmittance is 92.5% in 240 – 1350 nm. A collimeter of 40 mm aperture is used to make a four-fold laser beam dimension and a 1/4 beam divergence.

The receiving system is shown in Fig. 4. Backscattered light signal from the overhead sky is received with 50 cm diameter telescope of Newtonian type, and changed to an electric signal with a photomultiplier tube (Hamamatsu Photonics R1332) after passing through an optical filter (Hoya U-340). The signal is processed with a discriminator (PAR 1121), two photon-counters (PAR 1109), interface and CPU (DEC PDP-11/23), and finally stored in a magnetic disk. The details of operation of these elements were described by *Iwata et al. [1983]*. The reference time

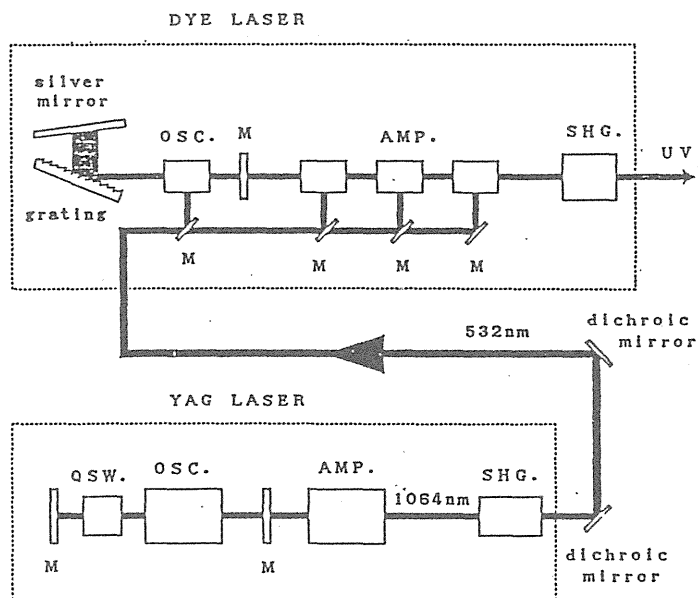


Fig. 1. Outline of laser installation.

OSC.: oscillator; AMP.: amplifier; QSW.: Q switch; M: mirror; SHG.: second harmonic generator

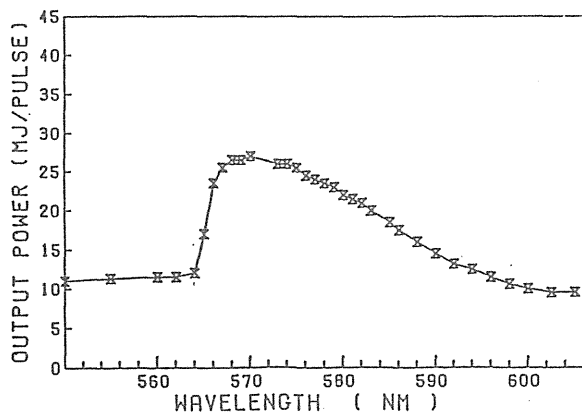


Fig. 2. Output power of dye laser fundamental.

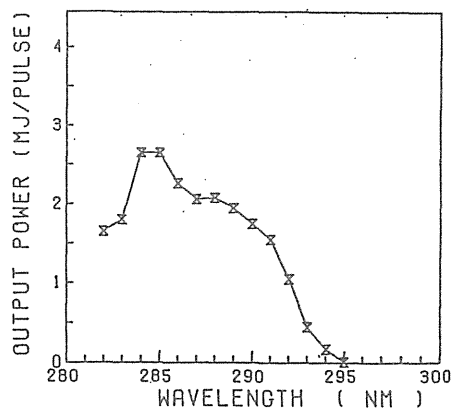


Fig. 3. Output power of dye laser second harmonic.

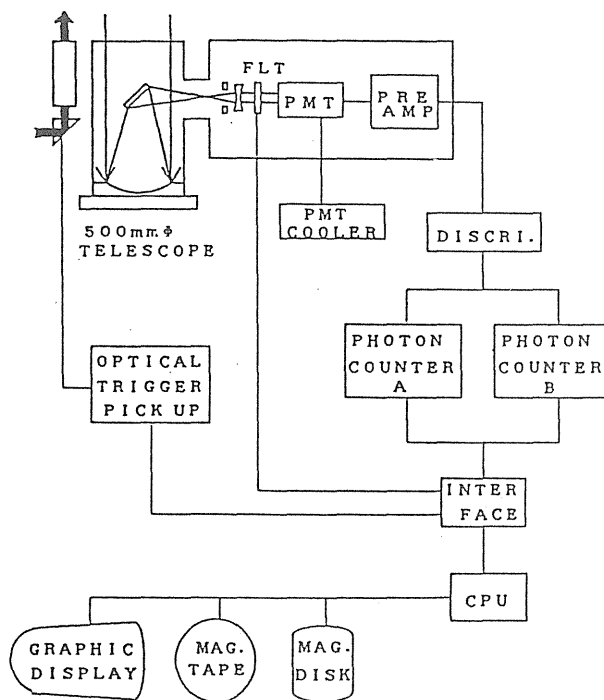


Fig. 4. Outline of receiving system.

FLT: optical filter; PMT: photomultiplier tube;
DISCRI.: discriminator

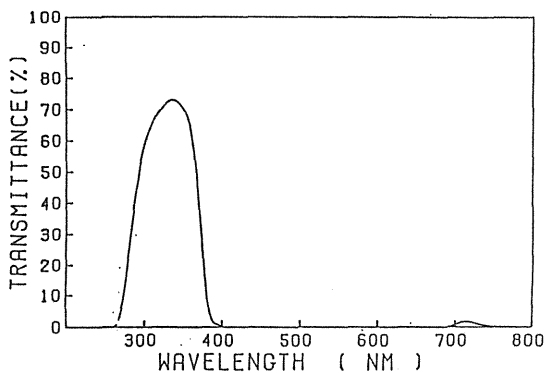


Fig. 5. Transmittance of optical filter inserted in front of PMT.

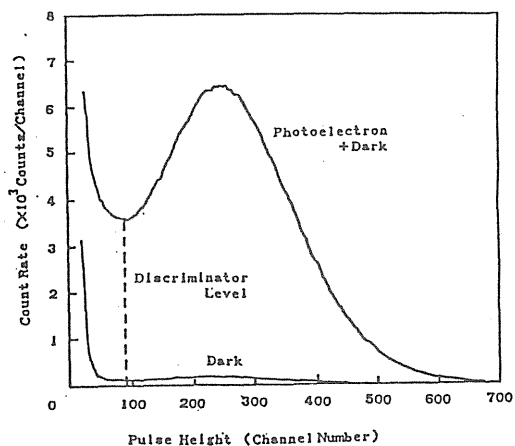


Fig. 6. Pulse height spectrum of PMT.
Supply voltage: 1640 V;
Light source: W lamp (400 nm);
Pulse height analyzer: Canberra Series 30;
Amplifier: Canberra 1K-200

Table 1. Laser specifications.

	Nd:YAG laser		Dye laser	
	fund.	2nd h.	fund.	2nd h.
Wavelength (<i>nm</i>)	1064	532	564-590	282-295
Output (<i>mJ/pulse</i>)	700	180	27 (at 570 <i>nm</i>)	2.7 (at 285 <i>nm</i>)
Repetition rate (<i>pps</i>)	10		10	
Pulse width (<i>ns</i>)	15		20	
Beam dimension (<i>mm</i>)	8		5	
Beam divergence (<i>mrاد</i>)	0.6		0.5	

to determine altitude of backscattering light is obtained with an optical trigger pickup (PAR 1301) mounted on the side of prism in the transmitting system. The measurable height range is in 128 height steps selected at every 0.3 – 1.8 *km* to give the height resolution. The lowermost height of measurement is selected at 0.8 – 30 *km*.

Figure 5 shows the wavelength characteristics of used optical filter, which cuts off extra light component other than necessary wavelength range. The radiant sensitivity of PMT is 35 *mA/W*, and the quantum efficiency is 15% at 285 *nm*. Figure 6 shows the pulse height spectrum of PMT. The discriminator is set at the level of about 90 (channel number) to minimize the dark current effect and to increase the signal to noise ratio.

3. Example of observation

Figure 7 is an example of observation at 284 *nm* for 10 minutes (6000 laser pulse shots) in midnight on December 28, 1987. The thick line is the actually measured photon count number, and the vertical broken line is the noise count measured at the same time. The net count number in thin solid line, which is the measured count subtracted by the noise count, corresponds to the backscattered signal. Since the dark current noise of PMT is confirmed to be less than 1 count for 3000 shots as shown in Fig. 8, almost all the noise component comes from background due to external light such as stars and scattered city lights.

Figure 9 shows the net count numbers of observations successively made at two wavelengths 284 *nm* (solid line, same as in Fig. 7) and 288 *nm* (broken line), with 300 *m* height resolution. The difference of the two curves corresponds to that of absorption cross-sections at the respective wavelengths. In this range of Hartley band the cross-section is smaller in the longer wavelength as shown in Fig. 10 [Ackerman, 1970].

If the two wavelengths used in the DIAL method are not appreciably apart from

each other, the effect of Rayleigh and Mie scatterings is almost canceled, and the term of differential absorption

is distinguished. Then the density of object material causing absorption, ozone in this case, between the height of R and $R + \Delta R$, is approximately given by

$$N(R + \frac{\Delta R}{2}) = \frac{1}{2\Delta R\{\sigma(\lambda_1) - \sigma(\lambda_2)\}} \log \frac{n(\lambda_1, R) \cdot n(\lambda_2, R + \Delta R)}{n(\lambda_2, R) \cdot n(\lambda_1, R + \Delta R)}$$

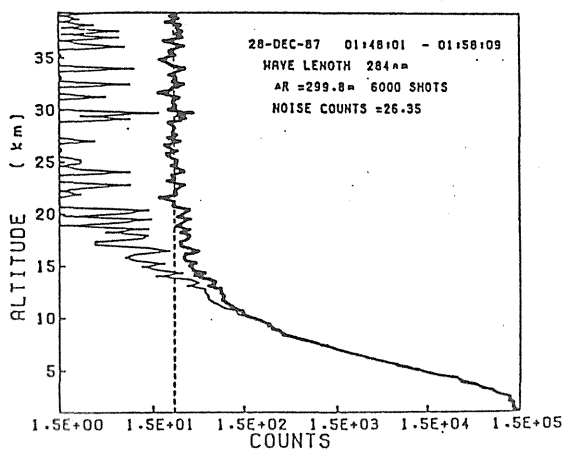


Fig. 7. Example of observed signal count at 284 nm.

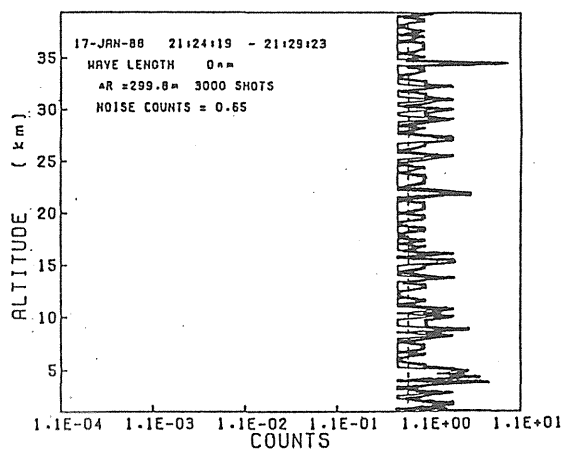


Fig. 8. Observed count for dark current noise.

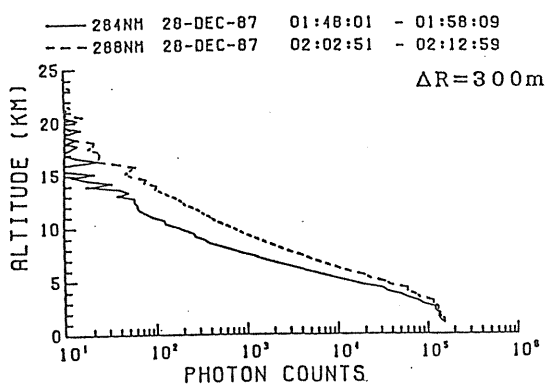


Fig. 9. Backscattered signal count in observations at 284 and 288 nm on Dec. 28, 1987.

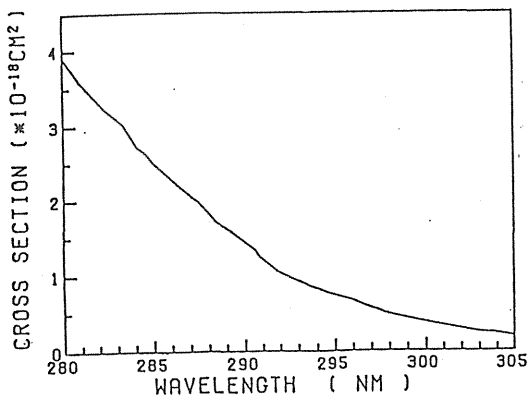


Fig. 10. Absorption cross-section of ozone in the wavelength range 280–305 nm.

where $\sigma(\lambda_i)$ is the absorption cross-section at wavelength λ_i ($i = 1$ and 2), and $n(\lambda_i, R)$ is the backscattered signal intensity received at wavelength λ_i and altitude R . Figure 11 is the vertical profile of ozone derived from the observations of Fig. 9 using the above equation and the ozone absorption cross-section shown in Fig. 10. In deriving the profile, the data of three successive intervals are running-averaged to minimize their fluctuation. The meaningful values were not obtained in the altitudes lower than 2 km because of strong scattering of aerosols, and upper than 8 km because of too weak signals.

Horizontal bars in Fig. 11 represent the error ranges at the respective altitudes, which are deduced from the consideration of shot noise in PMT. At about 7 km altitude the error range reaches the same order as the values of ozone density. For checking the reliability of the results, the model ozone profile [Krueger and Minzner, 1976] is also shown in Fig. 11 as black circles together with their standard deviations for temporal variations. It is widely recognized that the ozone density in the troposphere is very variable according to the meteorological or industrial conditions. Considering the extent of variation, the result of observation and reduction here is thought to represent the reasonable ozone profile at the time of observation without serious errors up to at least 6 km altitude.

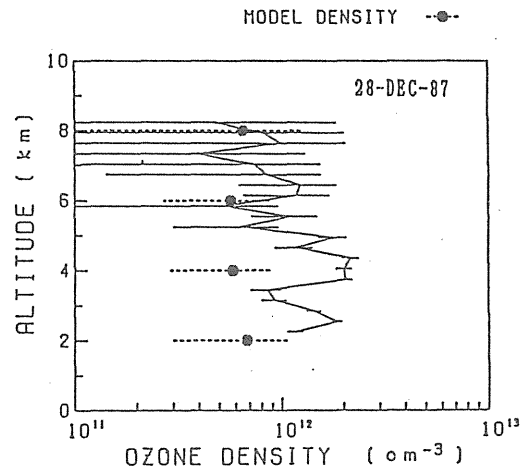
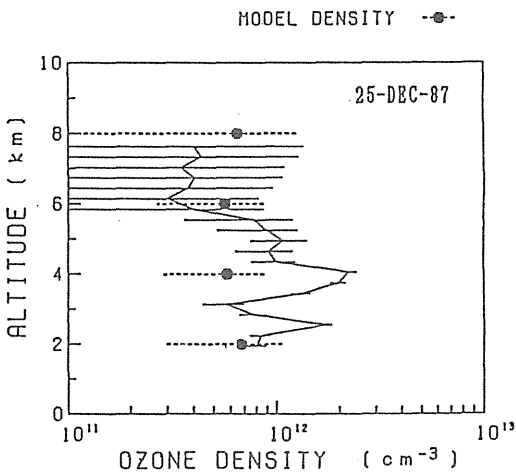


Fig. 11. Ozone profile obtained from the observations shown in Fig. 9. Error bars are estimated from the consideration of PMT shot noise. Model ozone density and the standard deviation are shown in black circles and broken bars.

$\lambda_1 = 284nm(6000 \text{ shots});$
 $\lambda_2 = 288nm(6000 \text{ shots})$

Fig. 12. Another example of ozone profile obtained on Dec. 25, 1987.

$\lambda_1 = 283nm(3000 \text{ shots});$
 $\lambda_2 = 289nm(3000 \text{ shots})$

Another example shown in Fig. 12, which was obtained from the observations for each 5 minutes on December 25, 1987 using the wavelengths 283 and 289 *nm*, gives the results similar to the above.

4. Conclusions

A preliminary experiment was made to construct a system for the monitoring of ozone profile. The procedures and results of experiment are summarized as follows. The characteristics of dye laser using Rh6G dye in methanol solvent were examined. After careful tuning, the laser output power usable for the observation was more than about 2 *mJ/pulse* in the wavelength range 283 – 290 *nm* in Hartley ozone UV absorption band. But this power level was considerably lower than that expected at the phase of system preparations.

By using the differential absorption method, it was confirmed that a pair of observations respectively for 10 minutes at 284 and 288 *nm*, or for 5 minutes at 283 and 289 *nm*, gave reliable values of ozone concentration in the altitudes from 2 to 6 *km* with 900 *m* height resolution. Estimation was made of the error density caused by shot noise from photomultiplier tube. The result showed that the ozone density derived from the present system was unreliable at altitudes over 6 *km*.

Extension of measurable altitude requires improvement of the backscattered signal to noise ratio. The approaches for realizing it will be, for example, basically to get higher laser power, to increase accumulating laser pulse shot numbers or accumulation time, and to find a better pair of observation wavelengths by using other kinds of dye. The increase of accumulation time, however, will require frequent shorter period changeovers between a pair of wavelengths, otherwise considerable errors may result from the changeable atmospheric conditions between the time difference of operation at the respective wavelengths. This fundamental modification is indispensable in laser and processing systems.

Acknowledgments

In preparing the system and carrying out the observations, the technical assistance by H. Jindo, M. Kanada, N. Toriyama, and M. Hori is very much appreciated.

References

- Ackerman, M., Ultraviolet solar radiation related to mesospheric processes, in *Mesospheric Models and Related Experiments*, ed. G.Fiocco, D.Reidel Publ. Co., 149-159, 1970.
- Browell, E.V., S. Ismail, and S.T. Shipley, Ultraviolet DIAL measurements of ozone profiles in regions of spatially inhomogeneous aerosols, *Appl. Opt.*, *24*, 2827-2836, 1985.
- Fishman, J., R.C. Whitten, and S.S. Prasad, *Ozone in the Free Atmosphere*, Van Nostrand Reinhold Company, 161-194, 1985.
- Iwata, A., Y. Kondo, and M. Takagi, A laser radar system for the observation of minor atmospheric constituents in the stratosphere, *Proc. Res. Inst. Atmos., Nagoya Univ.*, *30*, 25-35, 1983.
- Krueger, A.J. and R.A. Minzner, A mid-latitude ozone model for the 1976 U.S. Standard Atmosphere, *J. Geophys. Res.*, *81*, 4474-4481, 1976.
- Megie, G., G. Ancellot, and J. Pelon, Lidar measurements of ozone vertical profiles, *Appl. Opt.*, *24*, 3454-3463, 1985.
- Pelon, J. and G. Megie, Ozone monitoring in the troposphere and low stratosphere: evaluation and operation of a ground based lidar station, *J. Geophys. Res.*, *87*, 4947-4955, 1982.
- Schotland, R.M., Errors in the lidar measurement of atmospheric gases, *J. Appl. Meteor.*, *13*, 71-77, 1984.

